Free Volume After Cure vs. Fractional Conversion for a High-T_g Epoxy/Amine Thermosetting System

R. A. VENDITTI,[1] J. K. GILLHAM,[1,*] Y. C. JEAN,[2] and Y. LOU[2]

[1]Polymer Materials Program, Department of Chemical Engineering, Princeton University, Princeton, New Jersey 08544; [2]Department of Chemistry, University of Missouri at Kansas City, Kansas City, Missouri 64110

SYNOPSIS

Isothermal glassy-state properties of cured thermosetting materials pass through maximum and minimum values with increasing fractional chemical conversion. In this work, a diglycidyl ether of bisphenol A (a diepoxide) and trimethylene glycol di-*p*-aminobenzoate (a tetrafunctional aromatic diamine) system was investigated for the purpose of analyzing the complex behavior after cure of the isothermal properties of the glassy state with increasing conversion. The glass transition temperature (T_g) is used as a direct measure of conversion. Dilatometric, differential scanning calorimetry, torsional braid analysis, and positron annihilation spectroscopy techniques were used to monitor the density, T_g, modulus, and free volume of the material after cure with increasing conversion. The specific volume at 25°C after cure passes through a minimum and the modulus passes through a maximum with increasing conversion. The fractional free volume and the average radius of free volume at 25°C after cure pass through minimum values with respect to conversion. The specific volume, modulus, and fractional free volume at 25°C vs. conversion data qualitatively correlate. The anomaly of the increasing specific volume in the glassy state with increasing conversion is thus considered to arise from changes in free volume on a length scale corresponding to angstroms. The increasing free volume with increasing conversion is related to the phenomenon of antiplasticization. © 1995 John Wiley & Sons, Inc.

INTRODUCTION

The isothermal specific volume of the glassy state of a thermosetting material after cure has been observed to increase with increasing conversion.[1-6] This so-called anomaly has significant implications for the properties and performance of thermosetting materials. The increase in specific volume of the glassy state has been correlated with a decrease in modulus[7,8] and an increase in equilibrium water absorption.[9] It has been attributed to an increase in free volume on the basis of the magnitude of changes in modulus and water absorption.[1]

An example of the anomalous behavior is shown in Figure 1.[10] The material analyzed for the data in Figure 1, which is the material investigated for this report, is a stoichiometric mixture of a difunctional epoxy, a diglycidyl ether of bisphenol A (DGEBA), and a tetrafunctional aromatic diamine, trimethylene glycol di-*p*-aminobenzoate (TMAB). The modulus measured at 25°C vs. conversion (as measured by the glass transition temperature, T_g) is observed to display a maximum value with respect to T_g. T_g is used as a direct measure of conversion in Figure 1 and also in the main body of this report.[11-17]

The value of T_g corresponding to the maximum value of the modulus in Figure 1 is denoted as the end of the glass transition, ${}_eT_g$. The maximum value of the isothermal modulus at 25°C is considered to arise from the competition between the increase in modulus due to the glass transition temperature rising above the measurement temperature (T_{meas}) and the decrease due to the anomaly.

A conversion–temperature–property diagram (T_gTP diagram) for a thermosetting material can be used to map the trends in an isothermal property after cure vs. conversion.[7,8,10,17,18] A composite T_g TP diagram for four different stoichiometric ratios of

* To whom correspondence should be addressed.

Journal of Applied Polymer Science, Vol. 56, 1207–1220 (1995)
 CCC 0021-8995/95/101207-14

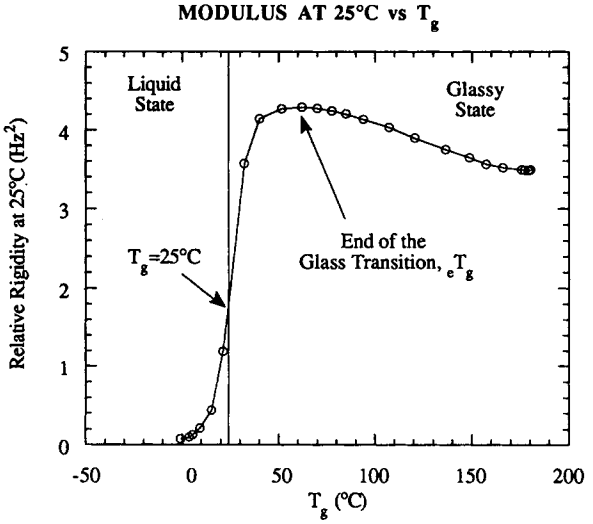

Figure 1 Modulus (~ relative rigidity) at 25°C after cure vs. conversion as measured by T_g. The maximum in the modulus is designated as the end of the glass transition. Gelation occurs at a conversion corresponding to T_g = 42°C. Vitrification, the change from the liquid or rubbery state to the glassy state, is defined as $T = T_g = 25$°C (solid vertical line). Data from Ref. 10.

TMAB to DGEBA is shown in Figure 2[10] and was constructed, in part, using data such as in Figure 1. Transition (relaxation) temperatures and values of the modulus were obtained using a torsional pendulum technique, i.e., torsional braid analysis.[19-21] This particular diagram uses T_g as a direct measure of conversion. The diagram includes the temperature values of the mechanical relaxations at approximately 1 Hz, i.e., the glass transition temperature ($T = T_g$, i.e., vitrification) and the sub-T_g glassy-state relaxation temperatures (T_β and T_γ). Maximum ($_eT_g$) and minimum values of the modulus with respect to conversion are included in Figure 2. The locus of maximum values in the isothermal modulus vs. conversion appears to be related to gelation at low conversions and related to vitrification ($T_g = T$) at higher conversions.[10]

The T_gTP diagram succinctly summarizes the behavior of the isothermal properties of the glassy state after cure vs. conversion. The diagram is useful in that the changes in properties after cure, e.g., changes in modulus, with respect to increasing conversion may be correlated with events such as gelation and vitrification and with the relationships of T_g and the sub-T_g glassy-state relaxation temperatures to the measurement temperature. In this study, the source of the anomaly of the increase in specific volume and the decrease in modulus after cure with increasing conversion after vitrification is investigated at the atomic length scale.

The main topic of this work focuses on the various contributions to the changing isothermal specific volume of a thermosetting material after cure with respect to conversion. The specific volume is a key property for analysis due to its influence on all other properties. For discussion, the specific volume of a material, V, is separated into two parts:

$$V = V_0 + V_f \tag{1}$$

where V_0 is the volume occupied by the covalently bound atoms, and V_f is the free volume or unoccupied volume. The occupied volume can further be separated:

$$V_0 = V_W + V_V \tag{2}$$

where V_W is the volume of the covalently bound atoms as defined by their van der Waals radii, and V_V, the added volume that the atoms exclude due to vibrations.[22] Note that V_f and V_W do not sum to V. It is assumed that V_V is constant with respect to conversion for a thermosetting system at a given tem-

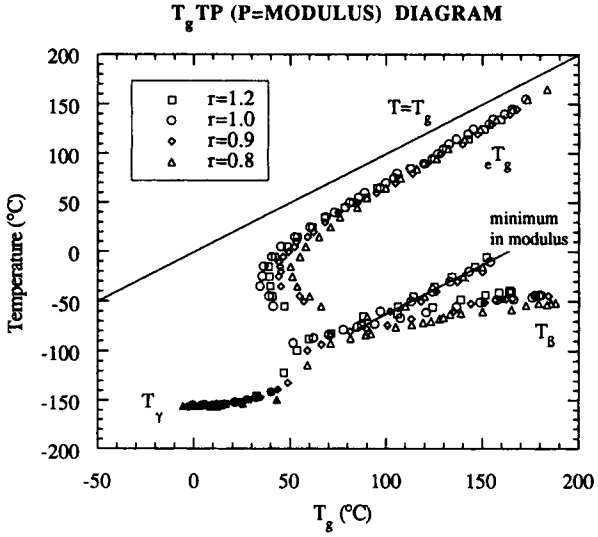

Figure 2 Conversion (T_g)–temperature–property diagram. Data for the DGEBA/TMAB system with four different ratios of amino hydrogen to epoxide (r) are plotted. $_eT_g$ marks the conversion, as measured by T_g, at which the modulus at an isothermal measurement temperature passes through a maximum value. The locus of the values of $_eT_g$ for each of the four systems displays a lower conversion limit which appears to correlate with the conversion at gelation. Data for T_g, T_β, T_γ, and the minimum in modulus vs. conversion are also included. Data from Ref. 10.

perature ($T < T_g$). Thus, changes in V_0 with conversion will be directly related to changes in V_W.

It is shown in this report that the calculated V_W vs. conversion behavior and the V vs. conversion behavior do not correlate. If V_0 (as reflected in V_W) vs. conversion behavior does not dominate the V vs. conversion behavior, then, according to eq. (1), anomalous changes in V should be attributed to anomalous changes in V_f. To test this assumption, the fractional free volume, V_f/V, is measured at 25°C on epoxy/amine specimens with different conversions using positron annihilation spectroscopy[23-26] and the values are compared to measured values of V vs. conversion data. It is a conclusion of this work that V_f and V both pass through a minimum value with respect to conversion for the thermosetting system and that the anomaly arises from the void content at the free-volume level.

EXPERIMENTAL

Chemical System

The chemical system was a diglycidyl ether of bisphenol A (DGEBA; DER332, Dow Chemical Co.) cured with a tetrafunctional aromatic diamime, trimethylene glycol di-*p*-aminobenzoate (TMAB; Polacure 740M, Air Products Co.). The chemical structure of the reactants and the dominant reactions of the system are shown in Figure 3. There is no mass loss associated with the reactions. The epoxy monomer is a viscous liquid at 25°C and has an epoxide equivalent weight (EEW) of 174.4 g/equiv (determined by bromine titration by Dow Chemical Co.; cf. theoretical EEW = 170 g/equiv for the pure chemical). The amine curing agent is a highly crystalline solid at 25°C (melting point = 125°C) with the theoretical amino hydrogen equivalent weight of 78.5 g/equiv.

A stoichiometric ratio of amino hydrogens to epoxide groups was used in this study, i.e., 1 mol of diamine to 2 mol of diepoxide. The chemical kinetics of the DGEBA/TMAB system have been investigated for formulations with a stoichiometric proportion of reactants,[11,27] an excess amine proportion,[16] and an excess epoxy proportion.[16] For the stoichiometric formulation, the only significant reactions are between the epoxide and the amino hydrogen (Fig. 3). T_gTP diagrams have been constructed for the stoichiometric and nonstoichiometric proportions of the diamine to the diepoxy.[7,8,10] Physical aging studies of the stoichiometric material have been reported for the fully cured material[28,29]

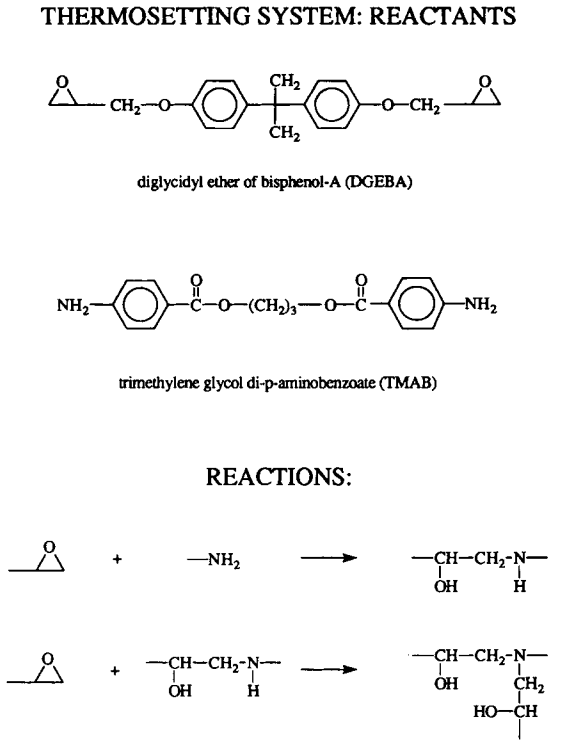

Figure 3 DGEBA/TMAB thermosetting system: reactants and reactions.

and vs. conversion for the partially cured material.[7,30] The work reported herein forms part of a PhD thesis.[29] A preliminary report has been published.[31]

Mixing Procedure

A stoichiometric amount of crystalline amine was added to the liquid epoxy monomer at 100°C. The mixture, approximately 50 g, was then vigorously stirred for 30 min. This procedure was adopted to ensure homogeneous mixing and to avoid the use of solvent, the presence of which could complicate investigation of the kinetics and properties vs. chemical structure.[11] Immediately after mixing, the warm liquid was degassed under vacuum ($\simeq$ 1 Torr) at 75°C for 15 min. The resulting clear viscous liquid was poured into numerous aluminum pans, which were individually sealed in plastic bags, kept in a dessicator, and stored in the freezer part of a refrigerator (the temperature of which was approximately −20°C).

Cure Procedure

The following procedure was followed for each maximum temperature of cure to produce specimens with different extents of cure: The initial reactive mixture

was removed from the freezer and allowed at least 20 min to reach room temperature before being taken out of its plastic bag (in order to prevent condensation of moisture onto the surface of the cold material). A portion of the mixture was poured into another aluminum pan and degassed in a vacuum oven for 15 min at 75°C (≃ 1 Torr). The degassed fluid mixture was used to fill a heated multicavity aluminum mold (50°C) that was lined with aluminum foil. The cavities resulted in disk-shaped specimens (average diameter approximately 5 mm; average thickness approximately 1 mm; average mass approximately 25 mg) which were to be used for measurements of density using a density gradient column and for measurements of fractional free volume and the radius of free-volume holes using positron annihilation spectroscopy. Part of the fluid mixture was also used to fill aluminum molds lined with aluminum foil that produced specimens of a rectangular form (width approximately 6 mm; length approximately 7 cm, thickness approximately 0.6 mm) for thermal expansion coefficient measurements. Part of the fluid mixture was also added to seven pans for analysis by differential scanning calorimetry (DSC). The DSC pans were filled and sealed under nitrogen. The average sample weight for the DCS analysis was approximately 10 mg.

The filled molds and filled DSC pans were then placed inside a temperature programmable oven at ambient temperature and pressure. The oven was purged continuously with nitrogen. The temperature was then raised at 5°C/m to a predetermined cure temperature, held isothermally at the cure temperature for 2 h, and then cooled at 5°C/min to 40°C. Cure temperatures ranged from 125 to 220°C. The molds and DSC pans were then removed from the oven.

At this juncture, the value of T_g of the specimens was determined (see later) using two of the sealed DSC pans (without debonding the specimens from the DSC pans). The rectangular specimens for thermal expansion coefficient measurements were peeled from the aluminum foil, placed in a dessicator, and stored in a freezer (for measurements at a later time after further treatment—see later). The disk specimens, or simply "disks," were removed from the aluminum foil and were inspected using a polarizing light microscope; all disks used for further study were free from visible voids, bubbles, and cracks that could affect the macroscopic density of the material.

The disks and remaining DSC specimens were then placed in a holding chamber designed to fit in a torsional braid analyzer (TBA; Plastics Analysis Instruments, Inc., Princeton, NJ) oven for further thermal treatment.[19–21] (The TBA oven is convenient because of the temperature control during both increasing and decreasing temperature ramps. The holding chamber was designed so that the disk specimens were allowed to freely contract and expand with changes in temperature. The TBA oven was continuously purged with dry helium.) The specimens were then heated at 5°C/m to 20°C above their previously DSC-determined T_g and then cooled at a controlled rate of 5°C/m to 25°C. The purpose of this additional thermal postcure treatment was to remove physical aging effects that may have occurred during cure and to relieve any stresses built up between the disk specimens and the aluminum foil. The disks were then inspected again under the polarizing light microscope. The disks and DSC pans were then either stored in a desiccator placed inside a freezer or used immediately for analysis.

Density Measurements

The densities at 25°C (24.95 ± 0.05°C) of the specimens after cure were measured using a density gradient column (ASTM D1505[32]) which had been prepared using toluene and carbon tetrachloride.[1,10] The column was calibrated with density floats of 1.21053, 1.21477, 1.21953, and 1.22447 g/cm^3. Density measurements of disk specimens commenced approximately 10 min after their removal at 25°C from the TBA oven. Two to four specimens with the same cure were added individually to the column at approximately 5 min intervals. The positions of the disks were recorded vs. time. The specimens, after an initial rapid decrease in height, equilibrated at a level in the column for a period of 1 h or more. The position at a time equal to 20 min after being placed in the column was used to determine the reported densities of the specimens. Reported densities are the average of the specimens tested.

DSC Measurements

An instrument (Perkin-Elmer DSC-4), equipped with an intercooler capable of cooling to −40°C, was used for all measurements. The DSC unit was purged continuously with dry nitrogen. The specimens (mass approximately 10 mg) were contained in weighed and sealed aluminum DSC pans. DSC measurements were performed on specimens after curing in the oven and also after thermal postcure treatment in the TBA oven (as above). A specimen, in its pan, was placed in the DSC unit at 25°C and cooled to −30°C at a programmed rate of 320°C/m. The specimen was then subjected to a temperature

scan from −30°C to approximately 50°C above its glass transition temperature, T_g, at a heating rate of 10°C/min.

DSC measurements were used to determine T_g, the extent of physical aging, and Δc_p (the heat capacity of the liquid or rubbery state minus that of the glassy state at T_g) of the specimens. The glass transition appears as an endothermic shift over a temperature interval in the DSC heating scan. In this study, T_g was defined as the midpoint of the step transition after removal of the aging effects. Δc_p was defined as the change in the heat capacity of the extrapolated liquid or rubbery state and the extrapolated glassy state vs. temperature data at the defined T_g after removing thermal aging peaks.

Physically aged specimens display an endothermic peak slightly above the T_g. No evidence of physical aging peaks was observed in the specimens using the postcure thermal treatment procedure described above.

Thermal Expansion Coefficient Measurements

Thermal expansion coefficients were determined below and above the T_g using gelled specimens, which could support the small applied load, and the capabilities of an automated dynamic mechanical analyzer for solid materials (Rheometrics Solid Analyzer RSAII). Rectangular specimens (dimensions approximately $0.6 \times 6 \times 23$ mm^3) were mounted at room temperature in the unit using the thin-film fixture. The atmosphere was flowing dry nitrogen. The specimens were then heated to approximately 20°C above the T_g (as determined from DSC scans) and then cooled to 30°C at 5°C/m. This ramp was intended to relieve stresses that may have arisen during the cure in the aluminum mold. The specimens were then heated to and cooled from $T_g + 20$°C at 5°C/m. The determination of the thermal expansion coefficients was made using the data during this cooling ramp. (It is noted that the temperature range used for measuring the expansion coefficient above T_g was small.) The value of T_g of each specimen was that taken using the corresponding DSC specimens. The instrument was programmed to keep the specimen under 10 g of tension (approximately 3×10^5 dyn/cm^2) during temperature ramps by automatic adjustment of the relative positions of the thin-film fixture clamps. (No dynamic mechanical characterization was performed.) The change in position of the clamps was recorded vs. temperature and used to determine changes in the length of the specimen and also the corresponding coefficients of linear and volumetric expansion.

Positron Annihilation Spectroscopy

Details of positron annihilation spectroscopy (PAS) have been presented in the literature.[23–26] Positron annihilation lifetime measurements provide information on the concentration and average dimensions of free-volume holes in amorphous materials. A positron, the antiparticle of an electron, is more stable in vacuum than in the bulk and therefore tends to exist in the free volume when within a solid. Specifically, the *ortho*-positronium, denoted as *o*-Ps, an electron bound to a positron, is used to determine free volume.

The *o*-Ps typically lives for 0.5–3 ns in the free-volume holes. The lifetime of an *o*-Ps is related to the size of free volume in which it exists. The conversion of lifetime data to free-volume hole size data has been discussed.[23] One assumption that is generally made in this calculation is that the free-volume holes are spherical. With this assumption, positron lifetime measurements have been calibrated to free-volume hole sizes by analyzing structures with known pore size.

The intensity of the *o*-Ps annihilation signal provides information on the fractional free volume of a material. Calibration of the *o*-Ps annihilation intensity vs. fractional free volume has been performed by analyzing samples with known fractional free volume.[23] Specifically, poly(ether ether ketone) with different amounts of crystallinity was analyzed. The crystalline regions display no free volume relative to the amorphous regions; the amorphous regions were assumed to have a fractional free volume of 0.025 at T_g. Thus, by performing PAS experiments on samples with crystallinity ranging from 0 to 30%, the intensity of the *o*-Ps annihilation signal vs. fractional free-volume relationship was obtained.

Note that the absolute magnitude of V_f/V from a PAS experiment is not known (due to the assumption that $V_f/V = 0.025$ at T_g in the above-described calibration procedure). However, relative values of V_f/V for different specimens may be compared; this allows free volume vs. chemical structure trends to be identified.

In this study, the value of V_f/V and the average radius of free volume at a temperature of 25°C were determined vs. fractional conversion. Disk-shaped specimens (the same type as used in the density measurements) were used for PAS experiments for specimens with $T_g > 25$°C. Samples in liquid form were used for specimens with $T_g < 25$°C. Specimens with $T_g < 25$°C were prepared by curing at 125°C in the liquid state for varying times (cf. specimens with $T_g > 25$°C which were cured for 2 h at cure temperatures ranging from 125 to 220°C).

Specimens were cured at Princeton University, placed in vials, and stored in a dessicator in a freezer. The specimens were then sent to the University of Missouri at Kansas City in vials in a dessicator within an insulated container containing dry ice. Total transit time was less than 24 h; all shipments contained dry ice upon arrival at the University of Missouri at Kansas City where they were stored in a dessicator in a freezer before being analyzed.

RESULTS AND DISCUSSION

Specific Volume vs. Conversion

The specific volume at 24.95 ± 0.05°C (from now on denoted as 25°C) vs. T_g is shown in Figure 4.

In a previous report from this laboratory,[1] two factors were identified that contribute to the specific volume at 25°C. The first factor, contributing to a *decrease* in volume at 25°C, is the decrease in volume with increased cure which is normally observed at cure temperatures $T_c > T_g$. The second factor, contributing to an *increase* in volume at 25°C with increased cure, is due to (a) higher T_g material contracting on cooling from T_c for a larger ΔT in the glassy state than in the liquid or rubbery state than does a lower T_g material and (b) the thermal expansion coefficient in the glassy state being less than in the liquid or rubbery state. Mathematically, this process can be described by the following:

$$V(T) = V(T_c) - E_l(T_c - T_g) - E_g(T_g - T) \quad (3)$$

where $V(T)$ is the volume at T; T_c, the cure temperature; and E_l and E_g, the slopes of the V vs. T data in the liquid or rubbery state and glassy state, respectively.[1] (A schematic diagram showing V vs. T for different values of T_g has been published.[1]) Differentiating with respect to fractional conversion of epoxy, x:

$$\frac{dV(T)}{dx} = \frac{dV(T_c)}{dx} + (E_l - E_g)\frac{dT_g}{dx} \quad (4)$$

or, equivalently, differentiating with respect to T_g:

$$\frac{dV(T)}{dT_g} = \frac{dV(T_c)}{dT_g} + (E_l - E_g) \quad (5)$$

The first term on the right-side of eq. (5) is usually negative and the second term is always positive.

The above argument is supported in this report with measured values for the two terms on the right side of eq. (5). For the DGEBA/TMAB system for conversions greater than $T_g = 80$°C (i.e., for gelled specimens), the first term on the right side of eq. (5) was measured to be -7.9×10^{-5} cc/g °C and the second term to be $+2.7 \times 10^{-4}$ cc/g °C. (The first term on the right side was calculated for a hypothetical cure temperature of 200°C. The calculation was based on the following measured quantities: the densities at 25°C, the values of E_l and E_g, and the values of T_g for specimens with $T_g > 80$°C.) Thus, the change in $V(T)$ at a given temperature with increased T_g is positive. This is in agreement with the V at 25°C vs. T_g data at conversions of $T_g > 80$°C shown in Figure 4. This is the observed macroscopic event that is the anomalous behavior. [For low conversions $|dV(T_e)/dT_g| > |(E_l - E_g)|$, which is responsible for the decrease in $V(T)$ with increasing conversion.] Further discussion in this work will focus on the molecular origins of this observed macroscopic behavior.

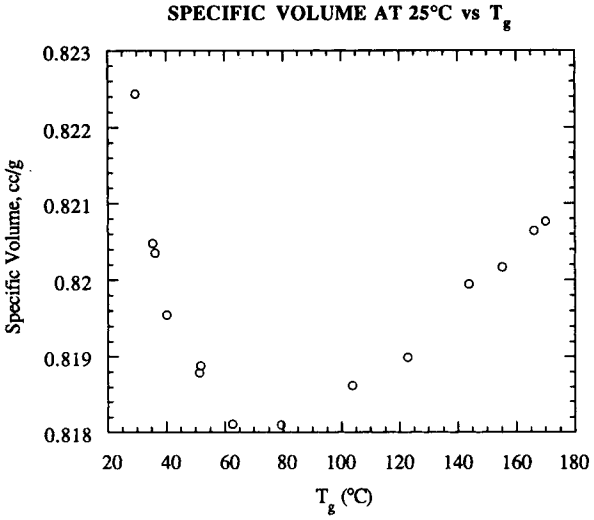

Figure 4 Specific volume at 25°C after cure vs. T_g.

Packing Density at 298 K vs. Conversion

It is of interest to probe the idea that the changing chemical structure of the thermosetting material changes the occupied volume of the molecules, which, in turn, dominates the anomalous trend in the specific volume. In this section, calculated changes in the van der Waals volume with respect to conversion are taken as an estimate of the changes in occupied volume. The van der Waals volume is then compared with the experimentally observed changes in specific volume.

The extent of structural packing in an amorphous material can be characterized by its packing density,

Table I Group Contributions to V_W : DGEBA/TMAB System

Group	V_W (cm^3/mol)	Source
$-C(CH_2)_2-$	30.67	Ref. 33, Table 14.1
$-CH_2-$	10.23	Ref. 33, Table 14.1
—O— (aromatic)	3.2	Ref. 33, Table 14.9
Phenyl-	43.32	Ref. 33, Table 14.4
Epoxide	20.71 − 1 = 19.71	Ref. 4
DGEBA	183.59	
$-NH_2$ (aromatic)	10.54 − 2 × 0.67 = 9.2	Ref. 33, Table 14.5
Phenyl-	43.32	Ref. 33, Table 14.4
—O(CO) (aromatic)	15.2	Ref. 33, Table 14.11
$-CH_2-$	10.23	Ref. 33, Table 14.1
TMAB	166.13	
—OH (aliphatic)	8.04 − 0.87 = 7.17	Ref. 33, Table 14.9
—CH—	6.78	Ref. 33, Table 14.1
$-CH_2CH(OH)-$	25.05 − 0.87 = 24.18	
Secondary $\diagdown\!\diagup$NH	8.08 − 0.67 = 7.41	Ref. 33, Table 14.5
Tertiary —N$\diagup\!\diagdown$	4.33	Ref. 33, Table 14.6

ρ^*, defined as the van der Waals volume divided by the total volume. The packing density is inversely related to the fractional free volume of a material. The packing density at 298 K may be calculated as follows:

$$\rho^*(298) = \frac{V_W}{V_T(298)} = \rho(298)\frac{V_W}{\mathrm{MW}} \qquad (6)$$

where V_W is the van der Waals volume of the "repeat unit" in cm^3/mol; V_T, the total volume (i.e., specific volume $\equiv V$) in cm^3/g mol; $\rho(298)$, the measured density at 298 K in g/cm^3; and MW, the molecular weight of the repeat unit in g/g mol (the basis of the calculation). For the DGEBA/TMAB system, the packing density is also affected by the fractional conversion of epoxide group (x):

$$\rho^*(x, 298) = \frac{V_W(x)}{V_T(x, 298)} = \rho(x, 298)\frac{V_W(x)}{\mathrm{MW}}$$

$$= \rho(T_g, 298)\frac{V_W(T_g)}{\mathrm{MW}} \qquad (7)$$

It has been previously shown that x is related in a one-to-one manner to the glass transition temperature, T_g, of the unaged DGEBA/TMAB system regardless of the cure temperature.[11,13] For this reason, T_g is used as an equally suitable parameter to characterize the extent of cure.

The van der Waals volume of the DGEBA/TMAB system is calculated by the method of group contributions.[33] Each portion of a molecule (e.g., a hydroxyl group) is assigned a contribution to the total van der Waals volume. The volumes of the different parts are then summed according to their frequency of occurrence, resulting in the total van der Waals volume in units of cm^3/g mol. Chemical reactions alter the structure of the material and therefore alter V_W. The reactions that occur in the DGEBA/TMAB system are (a) the epoxide group with primary amine to form a secondary amine and (b) the epoxide group with secondary amine to form a tertiary amine (see Fig. 3).

The group contributions of interest for unreacted DGEBA and TMAB molecules and for the species formed due to the reaction of epoxide with amine are summarized in Table I. V_W of the epoxide group has an approximated correction factor equal to −1 cm^3/mol due to its cyclic configuration relative to the corresponding linear species. Also shown in Table I are adjustments made for hydrogen bonding, which decreases V_W. The adjustments were made as follows: It is assumed in this calculation that any hydrogen attached to an oxygen or nitrogen will participate in hydrogen bonding. It has been shown that the distance of a hydrogen bond can be related to its infrared absorption peak wavenumber.[34,35] For the DGEBA/TMAB system, the hydrogen bonding of the hydroxyl and amino hydrogens have peak

wavenumbers at approximately 3505 and 3395 cm^{-1}.[27] These wavenumbers correspond to distances of the hydrogen bonds of the hydroxyl and amine hydrogen of 2.93 and 3.08 Å, respectively. Data published by Bondi (see curve I of Fig. 8.6, Ref. 33) can be used to determine the correction factors to V_W (as a function of the hydrogen bond distance) per hydrogen bond. They were determined to be −0.87 and −0.67 cm^3/mol for the hydroxyl and amino hydrogen, respectively. The larger negative correction factor of the hydroxyl hydrogen bond reflects the relative compactness of the hydroxyl hydrogen bond vs. the amine hydrogen bond.

The unreacted repeat unit is defined as 2 mol of DGEBA and 1 mol of TMAB and has V_W = 533.3 cm^3/mol and a molecular weight of 1011.6 g/g mol. This is the basis of the calculation. The van der Waals volume is calculated vs. the extent of reaction using the following expression:

$$V_W(x) = [2V_{W,E} + 1V_{W,A}] + 2[w_{2^0}\Delta V_W(1^0 \rightarrow 2^0) + w_{3^0}\Delta V_W(1^0 \rightarrow 3^0)] \quad (8)$$

where $V_W(x)$ is the van der Waals volume of the total system at fractional conversion x; $V_{W,E}$ and $V_{W,A}$, the van der Waals volume of unreacted DGEBA and TMAB, respectively; w_{2^0} and w_{3^0}, the mol fractions of secondary amino nitrogens and tertiary amino nitrogens of the total amino nitrogens, respectively; and $\Delta V_W\,(1^0 \rightarrow 2^0)$ and $\Delta V_W\,(1^0 \rightarrow 3^0)$, the changes in van der Waals volume of the system relative to the completely uncured material per existing secondary amine group and tertiary amine group, respectively, and equal to +2.68 and +4.07 cm^3/mol, respectively (from data in Table I). Note that both the reactions of the epoxide with primary amine and secondary amine lead to a net *expansion* of the van der Waals volume, +2.68 and +1.39 cm^3/mol, respectively. Ring opening of the epoxide dominates the calculated increases in V_W with increasing conversion.

Under the assumption of equal reactivity of the primary amine and secondary amine,[11,16,27] the mol fractions of secondary and tertiary amines were calculated as a function of fractional conversion, x, using the binomial random variable function:

$$w_{2^0} = 2x(1 - x) \quad (9)$$

$$w_{3^0} = x^2 \quad (10)$$

$$w_{1^0} = 1 - w_{2^0} - w_{3^0} \quad (11)$$

where w_{1^0} is the mol fraction of primary amine.

The fractional conversion of epoxide has been obtained experimentally by measuring the residual exotherm of a partially cured DGEBA/TMAB specimen in a DSC experiment.[11] The fractional conversion was calculated using the following expression:

$$x = \left(\frac{\Delta H_{\text{Total}} - \Delta H_{t,T}}{\Delta H_{\text{Total}}}\right) \quad (12)$$

where ΔH_{Total} and $\Delta H_{t,T}$ are the residual exotherms of the uncured and cured (for time, t, and cure temperature, T) material, measured on heating at 10°C/m, respectively. It has been stated that 100% fractional conversion is unlikely due to topological defects in the network structure.[36] However, in the present analysis, for convenience, the highest T_g recorded and the associated $\Delta H_{t,T}$ were considered to be "fully cured" properties.

It is convenient to determine the van der Waals volume in terms of T_g evaluated by DSC rather than the fractional conversion for a number of reasons.[11] These include that (a) T_g measured by DSC is more sensitive than is the fractional conversion at high fractional conversions (e.g., $x > 0.8$) due to the nonlinearity of the T_g vs. x relationship and (b) T_g is an important parameter in determining the physical state of the material. There is experimental evidence that T_g and x are uniquely related.[11–16] Therefore, it does appear to be valid to use T_g as a direct measure of cure.

Studies in this and other research groups have utilized theoretical models to relate T_g and x in thermosetting systems.[11–16,37] Of these, an equation proposed by Couchman to predict the T_g vs. compositional variation in linear polymer systems[38,39] was adapted to relate T_g and x in thermosetting systems[12]:

$$\ln(T_g) = \frac{(1 - x)\ln(T_{g0}) + \frac{\Delta c_{p\infty}}{\Delta c_{p0}} x \ln(T_{g\infty})}{(1 - x) + \frac{\Delta c_{p\infty}}{\Delta c_{p0}} x} \quad (13)$$

where Δc_p is the heat capacity of the liquid or rubbery state minus the heat capacity of the glassy state at T_g, and subscripts 0 and ∞ denote the uncured and fully cured specimen, respectively. It has been shown that eq. (13) successfully fits the data for the DGEBA/TMAB system as well as for other crosslinked systems and also for linear polyamic acid or ester to polyimide thermosetting systems.[12,40] The fit of eq. (13) to data[11] for the DGEBA/TMAB system is shown in Figure 5.

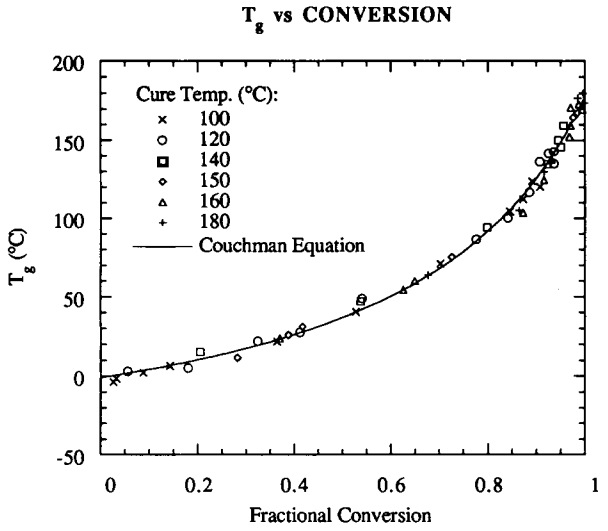

Figure 5 T_g vs. fractional conversion. The T_g vs. conversion behavior is independent of cure temperature. The modified Couchman equation adequately fits the data. Data from Ref. 11.

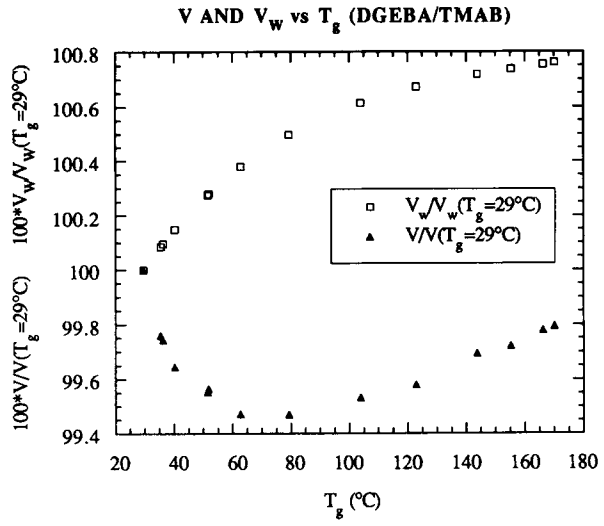

Figure 7 Specific volume at 25°C, V, and calculated van der Waals volume, V_W, vs. T_g for the DGEBA/TMAB system. Data are normalized with respect to values for T_g = 29°C.

By combining eqs. (8)–(13), an expression for V_W as a function of T_g results. The value of ρ^* (298 K) can then be calculated vs. T_g using eq. (7). Figure 6 shows ρ^* (T_g, 298 K) vs. T_g for the DGEBA/TMAB system. The macroscopic volume at 25°C passes through a minimum (Fig. 4) and the packing density at 25°C passes through a maximum (Fig. 6) with respect to conversion. However, since ρ^* incorporates both V_W and V, further discussion centers on V vs. conversion and V_W vs. conversion data independently, rather than ρ^* vs. conversion.

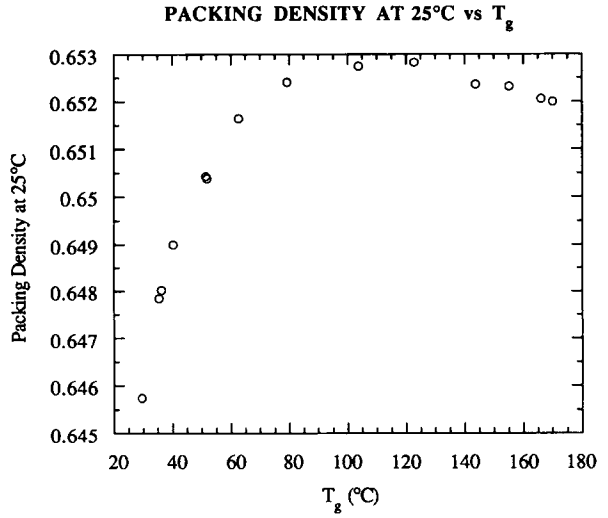

Figure 6 Packing density at 25°C vs. T_g. See text for details of calculation.

Comparison of van der Waals Volume and Specific Volume vs. Conversion

It is of interest to determine if the changes in V with conversion correlate with changes in V_W with conversion. V_W and V at 25°C, normalized with respect to their values for specimens with T_g = 29°C, are plotted vs. T_g in Figure 7. (The specimen with T_g = 29°C was the lowest-cured specimen for which the specific volume in the glassy state was measured.) At high conversion (T_g > 70°C), both V_W and V increase with increasing T_g. However, at values of T_g < 70°C, V_W increases but V decreases with increasing T_g.

The comparison of data in the T_g range where approximately 70 > T_g > 25°C may be affected by

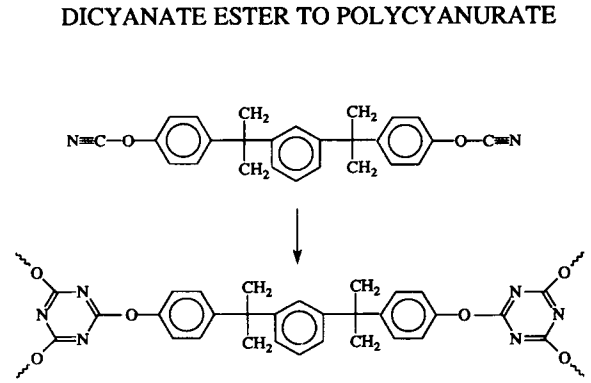

Figure 8 Dicyanate ester to polycyanurate thermosetting system: overall reaction.

Table II Group Contributions To V_W : Dicyanate Ester to Polycyanurate System

Group	V_W (cm³/mol)	Source
Cyanate	14.7	Ref. 33, Table 14.6
—O—	3.2	Ref. 33, Table 14.9
Phenylene	43.32	Ref. 33, Table 14.4
—C(CH₂)₂—	30.67	Ref. 33, Table 14.1
=C<	5.01	Ref. 33, Table 14.3
—N = (hetero, ar.)	5.2	Ref. 33, Table 14.6

the physical aging process at the measurement temperature, 25°C. The physical aging process involves the spontaneous densification of a glass at a temperature below its T_g in an attempt to achieve its equilibrium configuration.[7,28–30,41–44] The rate of physical aging generally becomes less as T_g-T increases.

The relationship between V_W and V vs. conversion is further analyzed herein using a dicyanate ester to the polycyanurate system. The overall reaction for this system is shown in Figure 8. The value of T_g of the unreacted material, T_{g0}, is −24°C and of the fully cured material is 185°C.[15] The polymerization (cure) kinetics of this system have been reported.[15] The specific volume at 25°C vs. fractional conversion data in Figure 9 have been obtained from Ref. 6. This particular system is convenient to analyze because (a) it is always at its stoichiometric ratio, which simplifies preparation and characterization, and (b) it does not have any hydrogen-bonding effects. Although it does not have any ring-opening reactions (as in the epoxide reaction), it does involve ring formation. V_W data are tabulated for the dicyanate ester to polycyanurate system in Table II.

For the dicyanate ester to polycyanurate system, V_W of an initial monomer unit (the basis of the calculation, or "repeat unit") is 227.1 cm³/mol. The same unit has a value of V_W = 217.45 cm³/mol in the fully cured state. From data in Ref. 33, it is approximated that a correction factor due to the cyclic ring formation is equal to −1 cm³/ring formed or −0.67 cm³/mol repeat unit. A net *contraction* from the uncured to the fully cured material corresponding to ΔV_W = −9.55 cc/mol per repeat unit (unlike the positive values for ΔV_W of the DGEBA/TMAB system) is calculated.

V_W and V, normalized with respect to the values at T_g = −24°C (the lowest conversion at which the volumetric data are available), are plotted vs. T_g in

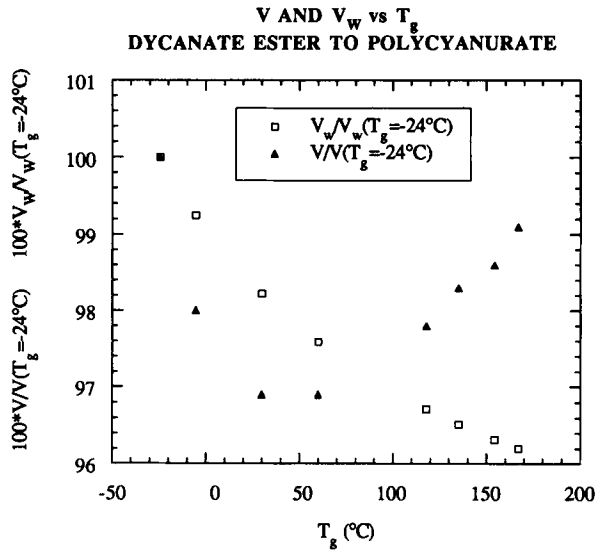

Figure 9 Specific volume at 25°C, V, and calculated van der Waals volume, V_W, vs. T_g for the dicyanate ester to polycyanurate system. Data are normalized with respect to values for T_g = −24°C. Specific volume vs. conversion data from Ref. 6. T_g vs. conversion data from Ref. 15.

Figure 9. Despite the net contraction of V_W throughout the entire range of T_g, V at 25°C of the dicyanate ester to polycyanurate system is observed to increase with increasing conversion for $T_g > 60$°C.

The measured specific volume vs. conversion for the DGEBA/TMAB and dicyanate ester to polycyanurate systems are qualitatively similar despite the different calculated V_W vs. conversion behavior. Thus, by using the DGEBA/TMAB and dicyanate ester to polycyanurate systems as examples, it is not

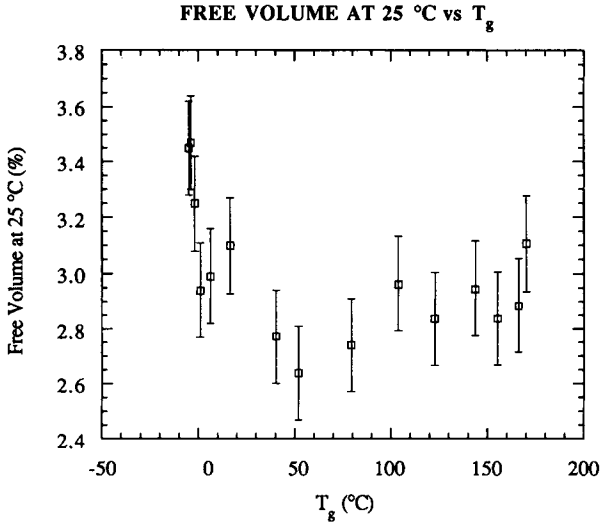

Figure 10 Free volume (%) at 25°C after cure vs. T_g.

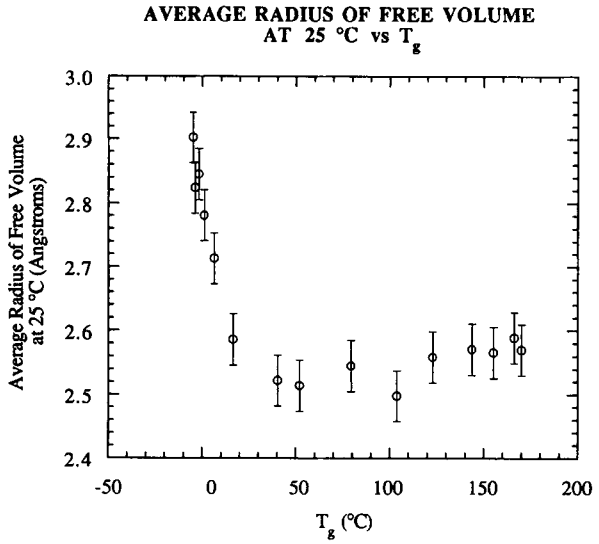

Figure 11 Average radius (Å) of free volume at 25°C after cure vs. T_g.

necessarily true that V vs. conversion behaves as does V_W vs. conversion. This suggests the changes in macroscopic volume vs. conversion are brought about by another factor, i.e., the free volume.

Free Volume vs. Conversion

The percent free volume and average free-volume hole size at 25°C vs. T_g are shown for the DGEBA/TMAB system in Figures 10 and 11, respectively. The free volume passes through a minimum vs. T_g. This is in accordance with the specific volume passing through a minimum vs. T_g and the packing density passing through a maximum vs. T_g. The correlation suggests that the changes in specific volume are a consequence of the changes in free volume vs. conversion.

The positron annihilation measurements provide results on the fractional free volume, V_f/V. The changes in the V_f/V vs. conversion can be attributed mainly to changes in the numerator, V_f, the actual free volume per mole of material, and not in changes in the denominator, the total volume, V. Evidence for this follows from a comparison of the magnitude of changes in V and V_f/V vs. conversion data. The increase in total volume of the material from its minimum volume at T_g = 70°C to its volume at T_g = 170°C is approximately 0.3% (Fig. 4). The increase in fractional free volume of the material from its minimum fractional free volume at T_g = 40–80°C to its fractional free volume at T_g = 170°C is approximately 17% (Fig. 10). The relatively small changes in total volume cannot account for the larger changes in fractional free volume. It is therefore concluded that the changes in fractional free volume, V_f/V, on the order of 17%, are due to changes in free volume, V_f, of approximately an equivalent magnitude.

The minimum in specific volume at 25°C occurs at a value of T_g equal to approximately 70°C (Fig. 4). The maximum in modulus at 25°C occurs at T_g equal to approximately 60°C (Fig. 1). The value of T_g at the minimum in fractional free volume at 25°C appears to be in the range of 40–80°C. In a qualitative sense, it can be concluded that the specific volume, modulus, and fractional free volume at 25°C all pass through extrema at approximately the same conversion.

The determination of free volume in the positron annihilation spectroscopy experiment is sensitive to physical aging; PAS experiments can reveal decreases in fractional free volume and increases in the average radius of free volume with physical aging.[23] The physical aging process may complicate the measurement of free volume for specimens with T_g slightly above the measurement temperature of 25°C. (The rate of physical aging increases dramatically as T_g–T decreases.) Specimens with small, positive values of T_g–25°C physically age to a larger extent during the PAS experiment performed at 25°C than specimens with higher values of T_g–25°C, which could complicate the results.

The length scale of the free volume detected in these samples is on the order of angstroms (Fig. 11). Evidence that the changes in specific volume correlate with changes on a length scale in the angstroms provides support that the increase in specific volume vs. conversion data is not due to events such as microbubbles or microcracks.

Antiplasticization

Antiplasticizers comprise a class of compounds that decrease the T_g as do plasticizers, but increase the modulus and decrease the elongation to break of certain glassy, polymeric (both linear and network) materials. The following discussion of antiplasticization, and how this process has a bearing on the properties of thermosetting systems vs. conversion, is based on Refs. 45–51.

When an effective antiplasticizer is added to a polymeric material, the following results for the glassy material: (a) The density of the antiplasticized material increases relative to that of the volume-averaged density of the polymer and antiplasticizer apart. (b) The shear and tensile moduli of the antiplasticized system increase relative to those of the

non-antiplasticized material. (c) The brittleness of the antiplasticized material increases relative to that of the non-antiplasticized material. (d) The intensities of the secondary (sub-T_g) relaxations of the antiplasticized material decrease relative to those of the non-antiplasticized material. (e) The diffusivity of gas molecules through the antiplasticized material decreases relative to that of the non-antiplasticized material. (f) The value of T_g of the antiplasticized material decreases relative to that of the non-antiplasticized material.

A compound may, in general, act like an antiplasticizer for a given polar polymer if the following requirements are fulfilled: (a) The polymer chains, or network, are relatively rigid and contain polar groups. (b) The antiplasticizer is a thin, polar, stiff molecule. (c) The antiplasticizer is compatible with the polymer, i.e., with no phase separation. (d) The concentration of the antiplasticizer is less than a critical value; each combination of antiplasticizer and polymer has a unique critical value for a given temperature. If the concentration of the "antiplasticizer" is greater than the critical value, then the compound acts as a plasticizer, decreasing both T_g and the modulus.

In general, three types of mechanisms of antiplasticization have been proposed: (a) induced crystallization, (b) the filling of free-volume holes with antiplasticizer, and (c) the hindrance of glassy state (sub-T_g) motions by the antiplasticizer. It seems reasonable that the proposed antiplasticization

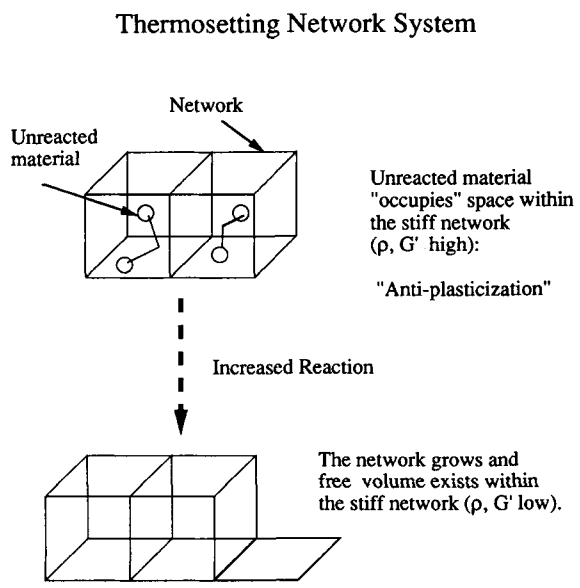

Figure 12 Schematic model of the antiplasticization process in thermosetting network systems (ρ = density, G' = modulus).

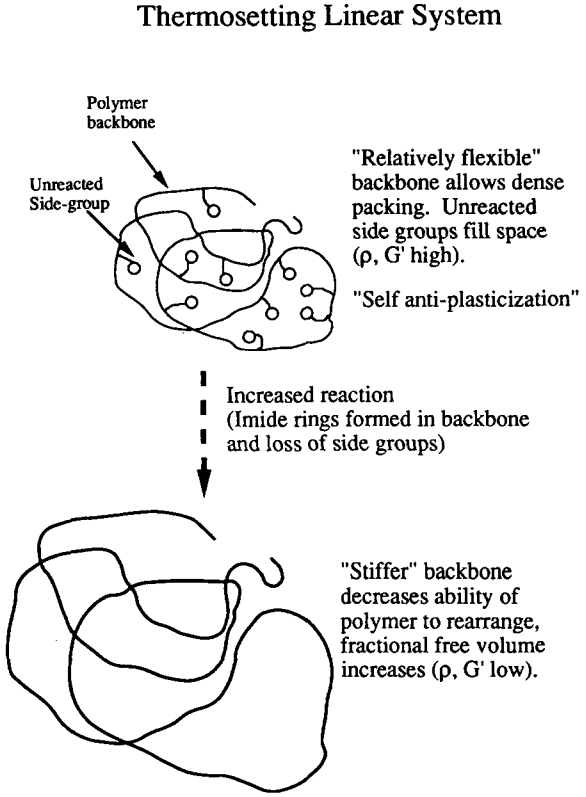

Figure 13 Schematic model of the antiplasticization process in thermosetting linear systems (ρ = density, G' = modulus).

mechanisms of (b) and (c) may be used to account for the so-called anomalous glassy-state isothermal properties vs. fractional conversion behavior of crosslinking systems such as DGEBA/TMAB[1,7,8,10,17] as well as for linear thermosetting systems such as linear polyamic acids (or esters) to polyimides.[18]

An alternative relaxational (i.e., kinetic) basis to the structural (i.e., packing) basis for the anomalous decrease in glassy-state isothermal density with increased cure has been discussed elsewhere.[1,10,17]

Figures 12 and 13 show schematically how antiplasticization relates to thermosetting systems vs. conversion. Imagine a hypothetical experiment where a fully cured network structure exists and where the network can be observed as the reactions that cause the crosslinks in the system are reversed (i.e., the fractional conversion decreases from $x = 1$). For the network system, as x decreases from 1, the system would contain a higher concentration of unreacted low molecular weight material and dangling, unreacted chain ends. These unreacted materials, defects in the network, meet the requirements for an effective antiplasticizer, as discussed above.

The effects of antiplasticization are observed experimentally in the DGEBA/TMAB system as the fractional conversion decreases. For example, for decreasing conversions from $T_g = 180$ to $T_g = 80°C$, the glassy-state modulus at 25°C increases (Fig. 1) and the density increases (or the specific volume decreases, Fig. 4). This suggests that the unreacted material is acting as a self-antiplasticizer.

Note that as x decreases further in Figure 4 the specific volume reaches a minimum. The minimum in volume with respect to conversion may be related to the critical concentration of antiplasticizer at 25°C; when x decreases to a certain value, the concentration of antiplasticizer (unreacted material) reaches its critical value for effective antiplasticization and further decreases in x cause typical plasticization of the material.

For the polyamic acid (or ester) to polyimide systems, the same comparisons between the antiplasticization process and the isothermal glassy state properties vs. conversion are valid[18]; however, for the polyimide systems, the reactive side groups act as an antiplasticizer for the linear polymer, which is stiff due to the existence of rings in the backbone structure.

The mechanism of unreacted material filling the free volume is supported by the increasing fractional free volume (or simply empty holes) at higher conversions (Fig. 10). The mechanism of the hindrance of glassy-state motions is supported by the thermomechanical results obtained at different conversions for the DGEBA/TMAB system (see Fig. 4, Ref. 8) as well as for the polyimide-type systems (see Fig. 2, Ref. 18).

Note that the effect that the changing polarity of the thermosetting system vs. conversion has not been discussed. It is reasonable to anticipate that changes in the polarity of the system with respect to chemical conversion will modify the properties of the system, such as modulus, concurrently with the process of antiplasticization.

CONCLUSIONS

1. The specific volume at 25°C passes through a minimum and the modulus passes through a maximum with increasing conversion (T_g) for the diepoxy cured with a tetrafunctional aromatic diamine material analyzed in this report.
2. Changes in the calculated van der Waals volume vs. conversion do not necessarily correlate with the behavior of the specific volume in the glassy state vs. fractional conversion for the thermosetting systems analyzed.
3. The fractional free volume and the average radius of free volume at 25°C pass through minimum values with respect to fractional conversion.
4. The specific volume, modulus, and fractional free volume at 25°C vs. conversion data qualitatively correlate.
5. The anomaly of the increasing specific volume and decreasing modulus after the conversion corresponding to vitrification is a consequence of an increase in submolecular fractional free volume with increase in conversion.
6. The increase in fractional free volume with increasing conversion may be related to the phenomenon of antiplasticization. In partially cured thermosetting systems, unreacted material may act as an antiplasticizer.

REFERENCES

1. K. P. Pang and J. K. Gillham, *J. Appl. Polym. Sci.*, **37,** 1969 (1989).
2. W. Fisch, W. Hofmann, and R. Schmid, *J. Appl. Polym. Sci.*, **13,** 295 (1969).
3. Y. G. Won, J. Galy, J. P. Pascault, and J. Verdu, *Polymer,* **32,** 79 (1991).
4. V. Bellenger, W. Dhaoui, and J. Verdu, *J. Appl. Polym. Sci.*, **33,** 2647 (1987).
5. A. Shimazaki, *J. Polym. Sci. C,* **23,** 555 (1968).
6. D. A. Shimp and S. J. Ising, in *35th International SAMPE Symposium and Exhibition,* Covina, CA, April 1990, Vol. 35(1), pp. 1045–1046.
7. X. Wang and J. K. Gillham, *J. Coat. Tech.*, **64,** 37 (1992).
8. X. Wang and J. K. Gillham, *J. Appl. Polym. Sci.*, **47,** 425 (1993).
9. M. T. Aronhime, X. Peng, and J. K. Gillham, *J. Appl. Polym. Sci.*, **32,** 3589 (1986).
10. R. A. Venditti and J. K. Gillham, in *Proceedings, Society of Plastics Engineers Conference,* New Orleans, 1993, Vol. 39, pp. 2336–2343; *J. Appl. Polym. Sci.*, **56,** 1687 (1995).
11. G. Wisanrakkit and J. K. Gillham, *J. Appl. Polym. Sci.*, **41,** 2885 (1990). Also: G. Wisanrakkit and J. K. Gillham, *J. Appl. Polym. Sci.*, **42,** 2453 (1991).
12. R. A. Venditti and J. K. Gillham, *Proc. ACS Polym. Mater. Sci. Eng. Div.*, **69,** 434–435 (1993).
13. X. Wang and J. K. Gillham, *J. Appl. Polym. Sci.*, **45,** 2127 (1992).
14. A. Hale, C. W. Macosko, and H. Bair, *Macromolecules,* **24,** 2610 (1991).
15. S. L. Simon and J. K. Gillham, *J. Appl. Polym. Sci.*, **47,** 461 (1993).

16. S. L. Simon and J. K. Gillham, *J. Appl. Polym. Sci.*, **46,** 1245 (1992).
17. S. L. Simon and J. K. Gillham, *J. Appl. Polym. Sci.*, **51,** 1741 (1994).
18. R. A. Venditti, J. K. Gillham, E. Chin, and F. M. Houlihan, in *Advances in Polyimide Science and Technology,* C. Feger, Ed., Technomic, Lancaster, PA, 1992, pp. 336–350.
19. J. K. Gillham, in *Developments in Polymer Characterisation,* J. V. Dawkins, Ed., Applied Science, London, 1982, pp. 157–227.
20. J. B. Enns and J. K. Gillham, in *Computer Applications in Applied Polymer Science,* T. Provder, Ed., ACS Symposium Series 197, American Chemical Society, Washington, DC, 1982, pp. 329–352.
21. J. K. Gillham and J. B. Enns, *Trends Polym. Sci.*, **2,** 406–419 (1994).
22. J. D. Ferry, *Viscoelastic Properties of Polymers,* Wiley, New York, 1970.
23. Y. C. Jean, *Microchem. J.*, **42,** 72 (1990).
24. D. M. Schrader and Y. C. Jean, Eds., *Positron and Positronium Chemistry,* Elsevier, Amsterdam, 1988.
25. Q. Deng and Y. C. Jean, *Macromolecules,* **26,** 30 (1993).
26. Q. Deng, F. Zandiehnadem, and Y. C. Jean, *Macromolecules,* **25,** 1090 (1992).
27. X. Wang and J. K. Gillham, *J. Appl. Polym. Sci.*, **43,** 2267 (1991).
28. G. Wisanrakkit and J. K. Gillham, *J. Appl. Polym. Sci.*, **42,** 2465 (1991).
29. R. A. Venditti, PhD Thesis, Department of Chemical Engineering, Princeton University, June 1994.
30. X. Wang and J. K. Gillham, *J. Appl. Polym. Sci.*, **47,** 447 (1993).
31. R. A. Venditti, J. K. Gillham, Y. C. Jean, and Y. Lou, *Proc. ACS Polym. Mater. Sci. Eng. Div.*, **71,** 815–816 (1994).
32. ASTM Standards, Part 27, ASTM, Philadelphia, 1965, p. 500.
33. A. Bondi, *Physical Properties of Molecular Liquids, Crystals and Glasses,* Wiley, New York, 1968.
34. K. Nakamoto, M. Margoshes, and R. E. Rundle, *J. Am. Chem. Soc.*, **77,** 6480 (1955).
35. G. C. Pimentel and A. L. McClellan, *The Hydrogen Bond,* Freeman, San Francisco, 1960.
36. E. F. Oleinik, in *Advances in Polymer Science,* Vol. 80, *Epoxy Resins and Composites IV,* K. Dusek, Ed., Springer-Verlag, Berlin, 1986, pp. 49–99.
37. M. T. Aronhime and J. K. Gillham, *J. Coat. Tech.*, **56,** 35 (1984).
38. P. R. Couchman and F. E. Karasz, *Macromolecules,* **11,** 117 (1978).
39. P. R. Couchman, *Polym. Eng. Sci.*, **24,** 135 (1984).
40. R. A. Venditti, J. K. Gillham, E. Chin, and F. M. Houlihan, *J. Appl. Polym. Sci.*, **53,** 455–461 (1994).
41. L. C. E. Struik, *Physical Aging in Amorphous Polymers and Other Materials,* Elsevier, Amsterdam, 1978.
42. R. A. Venditti and J. K. Gillham, *J. Appl. Polym. Sci.*, **45,** 1501 (1992).
43. R. A. Venditti and J. K. Gillham, *J. Appl. Polym. Sci.*, **45,** 501 (1992).
44. Z. H. Ophir, J. A. Emerson, and G. L. Wilkes, *J. Appl. Phys.*, **49,** 5032 (1978).
45. L. M. Robeson and J. A. Faucher, *J. Polym. Sci. Polym. Lett.*, **7,** 35 (1969).
46. W. J. Jackson, Jr. and J. R. Caldwell, *J. Appl. Polym. Sci.*, **11,** 211 (1967).
47. W. J. Jackson, Jr. and J. R. Caldwell, *J. Appl. Polym. Sci.*, **11,** 227 (1967).
48. M. D. Sefcik, J. Schaefer, F. L. May, D. Raucher, and S. M. Dub, *J. Polym. Sci. Polym. Phys. Ed.*, **21,** 1041 (1983).
49. N. Kinjo and T. Nakagawa, *Polym. J.*, **4,** 143 (1973).
50. J. Daly, A. Britten, A. Garton, and P. D. McClean, *J. Appl. Polym. Sci.*, **29,** 1403 (1984).
51. P. D. McClean, A. Garton, W. T. K. Stevenson, and K. E. MacPhee, *Polym. Compos.*, **7,** 330 (1986).

Received January 17, 1994
Accepted October 1, 1994